Eur Biophys J (2009) 38:329–338
DOI 10.1007/s00249-008-0325-9

OpenAccess

ORIGINAL PAPER

Inter-subunit disulfide cross-linking in homomeric and heteromeric P2X receptors

Benjamin Marquez-Klaka · Jürgen Rettinger · Annette Nicke

Received: 30 January 2008 / Revised: 31 March 2008 / Accepted: 2 April 2008 / Published online: 22 April 2008

Abstract P2X receptors are ATP-gated cation channels and assembled as homotrimers or heterotrimers from seven cloned subunits. Each subunit contains two transmembrane domains connected by a large extracellular loop. We have previously shown that replacement of two conserved residues, K68 and F291, by cysteine residues leads to disulfide cross-linking between neighbouring $P2X_1$ subunits. Since mutation of these residues results in a reduced ATP potency and cysteine cross-linking is prevented in the presence of ATP, we suggested an inter-subunit ATP binding site. To investigate whether the proximity of these residues is preserved in other P2X subtypes, we tested for spontaneous cystine formation between the corresponding $P2X_2$ (K69C, F289C), $P2X_3$ (K63C, F280C), and $P2X_4$ (K67C, F294C) mutants upon pairwise expression in *Xenopus laevis* oocytes. Non-reducing SDS-PAGE analysis of the purified receptors revealed a specific dimer formation between $P2X_2$K69C and $P2X_2$F289C mutants. Likewise, co-expression of $P2X_1$K68C and $P2X_2$F289C, but not $P2X_1$F291C and $P2X_2$K69C, mutants resulted in dimer formation between the respective subunits. Cross-linked $P2X_{1/2}$ heteromers showed strongly reduced or absent function that was selectively recovered upon treatment with DTT. Cross-linking was less efficient between $P2X_3$ or $P2X_4$ mutants but could be enhanced by the short cysteine-reactive cross-linker MTS-2-MTS. These results show that the spatial proximity and/or orientation of residues analogous to positions K68 and F291 in $P2X_1$ are preserved in $P2X_2$ receptors and at one of two possible interfaces in heteromeric $P2X_{1/2}$ receptors but appears to be redundant for $P2X_3$ and $P2X_4$ receptor function.

Keywords ATP binding site · Disulfide cross-linking · Subunit interface · Heteromerization

Abbreviations

P2XR	P2X Receptor
nAChR	Nicotinic acetylcholine receptor
iGluR	Ionotropic glutamate receptor
WT	Wild type
MTS-2-MTS	1,2-Ethanediyl-bismethanethiosulfonate

Introduction

Extracellular ATP is an autocrine and paracrine messenger molecule as well as a neurotransmitter. P2X receptors (P2XRs) are ATP-activated non-selective cation channels with a high Ca^{2+} permeability. Besides cys-loop receptors [comprising nicotinic acetylcholine receptors (nAChRs), serotonine receptor subtype 3, glycine receptors, and $GABA_A$ and $GABA_C$ receptors] and ionotropic glutamate receptors (iGluRs, comprising AMPA, kainate and NMDA receptors), P2XRs represent a third major family of neurotransmitter-gated ion channels. For both the tetrameric iGluR and the pentameric nAChR families the molecular structure of their agonist binding sites has been obtained by the X-ray structural analysis of soluble proteins with high homology to the respective agonist binding sites.

EBSA Satellite Meeting: Ion channels, Leeds, July 2007.

B. Marquez-Klaka · A. Nicke (✉)
Department of Neurochemistry,
Max-Planck-Institute for Brain Research,
Deutschordenstr. 46, 60528 Frankfurt, Germany
e-mail: anicke@gwdg.de

J. Rettinger
Department of Biophysical Chemistry,
Max-Planck-Institute of Biophysics,
Max-von-Laue-Str. 3, 60438 Frankfurt, Germany

The subunits of the cys-loop receptor family contain a large extracellular N-terminus followed by four transmembrane domains (TM1–TM4) with a large intracellular loop between TM3 and TM4. A molluscan ACh-binding protein resembles the extracellular N-terminal domain of the nAChR and other members of the cys-loop receptor family and likewise forms pentamers. Its crystal structure confirmed that the agonist binding pocket of this receptor family is formed at the interface of two neighbouring subunits by three loop-like structures from the principal (α-) subunit (A–C) and three β-strands from the complementary (β-) subunit (D–F) (Brejc et al. 2001). The principal (+) face of both the nAChR and AChBP binding pocket contributes five conserved aromatic side chains, a backbone carbonyl oxygen and a vicinal disulfide bridge located at the tip of the flexible loop C. The complementary (−) face is formed by more variable, mostly hydrophobic side chains. The flexible loop C is covering this binding pocket, and a closing movement of this loop upon agonist binding is assumed to initiate the conformational rearrangements that lead to channel opening (Hansen et al. 2005).

Subunits of the tetrameric ionotropic GluR family show a characteristic modular organization including an amino-terminal domain (ATD), three transmembrane domains (M1, M3 and M4), a re-entry loop (M2) which lines the lumen of the ion channel, and an intracellular carboxy-terminal domain. The agonist-binding sites of both metabotropic and ionotropic glutamate receptors show homology to bacterial periplasmic amino acid binding proteins. Using these as a template for the design of soluble iGluR ligand-binding domains, crystal structures for multiple "receptor"–ligand complexes were obtained (for reviews see Mayer 2006; Gouaux 2004). In contrast to the agonist binding sites of the cys-loop receptor family, the glutamate binding site of the ionotropic GluR is located within a single subunit between two separate extracellular segments, S1 (between TM1 and ATD) and S2 (between TM3 and TM4). The two segments are supposed to close in a "venus-flytrap"- or "clam-shell"-like mechanism upon agonist binding, thereby initiating the conformational changes necessary for channel opening. An arginine side chain (on helix D in S1) is essential for the high affinity binding of the α-carboxyl group of the ligand while the α-amino group of the ligand is bound by a conserved acidic side chain (on a loop prior to helix I on S2). iGluR subtypes differ in the number of water molecules necessary for coordinating the ligand, which is reflected in the variable size of the ligand binding pocket (Mayer 2005, 2006; Gouaux 2004).

A single P2X subunit contains two transmembrane domains linked by a large extracellular loop (North 2002), and a functional P2X receptor has been shown to consist of three subunits (Nicke et al. 1998; Barrera et al. 2005). An additional structural feature is ten conserved cysteine residues in the extracellular loop, which are arranged in two domains from C117 to C165 (six cysteine residues) and from C217 to C270 (four residues), respectively ($P2X_1$ sequence numbering). There is evidence that most, if not all ten cysteine residues form disulfide bridges within these domains (Clyne et al. 2002; Ennion and Evans 2002). Very recently, crystallization of the acid sensing ion channel 1 subtype (ASIC1), a member of the degenerin and epithelial sodium channel family, also revealed a trimeric structure (Jasti et al. 2007). Besides their quaternary structure, these ion channels share a common membrane topology with the P2XRs and likewise show a highly conserved but distinct arrangement of cysteine residues. However, the absence of a common cysteine pattern or conserved amino acid motifs between these ion channel families makes homology modelling of P2X receptors unlikely. Since no protein with sequence homology to P2X receptors has been identified, the information about its agonist-binding site is mainly based on mutagenesis studies.

Based on a model derived from secondary structure predictions, it has been proposed that the second half of the extracellular loop is folded similar to aminoacyl t-RNA synthetases (Freist et al. 1998) and harbours the ATP binding site. This hypothesis is supported by a mutagenesis study on $P2X_4$ receptors (Yan et al. 2005). Alanine substitution of conserved positively charged amino acid residues identified three lysine residues (K68, K70, and K309 in $P2X_1$) that are important for a high ATP potency in $P2X_1$ and $P2X_2$ receptors and were suggested to interact with the negatively charged phosphate chain of the ATP molecule (Ennion et al. 2000; Jiang et al. 2000). These results have partly been confirmed at $P2X_3$, $P2X_4$, and $P2X_7$ receptors (Wilkinson et al. 2006; Zemkova et al. 2007; Worthington et al. 2002). A recent single channel analysis on the background of a spontaneously opening $P2X_2$ mutant provides good evidence that at least K68 contributes directly to ATP binding while residues corresponding to K309 are more likely to have a function in channel gating (Cao et al. 2007). In addition, a conserved arginine residue (R292) and conserved aromatic amino acid residues (F185, F291), in particular, the conserved NFR motif (N290-R292 in $P2X_1$) has been supposed to contribute to ATP binding, possibly by interacting with the adenine ring (Roberts and Evans 2004, 2007). We have shown before that K68 and F291 of neighbouring $P2X_1$ subunits are in close proximity (Marquez-Klaka et al. 2007), suggesting an intersubunit binding site, similar as in nAChRs. This conclusion is supported by a functional study suggesting that K69 (corresponding to K68 in $P2X_1$) and K308 from neighbouring $P2X_2$ subunits contribute to ATP binding (Wilkinson et al. 2006).

To date, seven mammalian P2X subtypes have been cloned ($P2X_{1-7}$). Like in other ion channel families, functional and pharmacological diversity of P2X receptors is

increased by heteromerization of subunits. It is generally assumed that the arrangement of residues critical for receptor function is preserved in different channel subtypes. In this study, we used site-directed disulfide cross-linking to investigate whether the close proximity between residues homologous to K68 and F291 in $P2X_1$ is preserved in other P2X subtypes.

Materials and methods

cDNA constructs and cRNA synthesis

Construction of N-terminal hexahistidyl-tagged rat $P2X_1$ (His-$P2X_1$) cDNAs in the pNKS2 oocyte expression vector has been described previously (Nicke et al. 1998). Rat $P2X_2$, $P2X_3$ and $P2X_4$ clones were friendly provided by Dr. F. Soto (MPI for Experimental Medicine, Göttingen). The respective sequences were N-terminally His-tagged by PCR and subcloned into pNKS2, in an identical context as the His-$P2X_1$ sequence.

Site-directed mutagenesis was performed with the QuickChange mutagenesis Kit (Stratagene, La Jolla, CA, USA). Primers for cloning and mutagenesis were synthesized by MWG Biotech AG (Ebersberg, Germany). Sequences of all the constructs were verified by dideoxynucleotide sequencing (MWG Biotech AG). Capped cRNA was synthesized from linearized templates with SP6 RNA polymerase using the Message Machine kit (Ambion, Austin, TX, USA).

Protein biochemistry

Xenopus laevis toads were obtained from Nasco International (Fort Atkinson, WI, USA). Oocytes were prepared as previously described (Nicke et al. 1998) and, if not otherwise noted, injected with 50 nl aliquots of cRNA (0.5 µg/µl). To obtain similar amounts of surface labelled protein and to optimize the cross-link efficiency, cRNA ratios were adjusted to account for the different expression levels of the mutants. cRNA-injected oocytes and non-injected control cells were metabolically labelled by overnight incubation at 19°C with L-[^{35}S]-methionine at ~100 MBq/ml with ~0.1 MBq/oocyte (Perkin Elmer Life and Analytical Sciences, Rodgau-Jügesheim, Germany) in sterile ND96 (96 mM NaCl, 2 mM KCl, 1 mM $CaCl_2$, 1 mM $MgCl_2$ and 5 mM HEPES, pH 7.4) supplemented with gentamycin (50 µg/ml, Sigma, Taufkirchen, Germany), and subsequently kept for 48 h in 10 mM unlabelled methionine in ND96. For speciWc labelling of plasma membrane proteins, intact oocytes were incubated for 30 min in 50 lM Cy5-NHS-ester (GE Healthcare, Munich, Germany) in sterile ND96 (pH 8.5) 3 days after injection. Cysteine-speciWc cross-linking was carried out prior to surface labelling by a 10 min incubation in 100 lM 1,2-ethanediyl-bismethanethiosulfonate (MTS-2-MTS, Toronto Research Chemicals, North York, Canada) in ND96 (pH 8.5). To obtain comparable amounts of membrane bound receptors, expression times of the mutants were adapted. Oocytes were subsequently extracted as described previously (Marquez-Klaka et al. 2007), except that 50 mM iodoacetamide (Sigma, Taufkirchen, Germany) were added to the solubilization buVer, and 10 mM iodoacetamide to the washing buVer, to reduce unspeciWc cross-linking.

Blue native PAGE and SDS-PAGE were carried out as described (Schägger et al. 1994; Nicke et al. 1998; Marquez-Klaka et al. 2007). To account for variations in the amount of loaded protein, protein bands were quantified, and the amount of dimer was expressed as percentage of the total amount of P2X protein [monomer, dimer and (if present) trimer bands]. Gel documentation, analysis and band quantification were done on a Typhoon Trio Fluorescence Scanner (GE Healthcare, Munich, Germany) using the ImageQuant software (GE Healthcare, Munich, Germany). Experiments were repeated at least three times and similar results were obtained. Data are presented as mean ± SE.

Electrophysiological recordings

Current responses to ATP were measured 1–3 days after cRNA injection into *X. laevis* oocytes by using the two-electrode voltage-clamp technique. The standard solution used to superfuse the oocytes contained 90 mM NaCl, 1 mM KCl, 2 mM $MgCl_2$, and 5 mM HEPES, pH 7.4 (Mg^{2+} Oocyte Ringer). Calcium salts were omitted to avoid activation of endogenous Ca^{2+}-activated Cl^- channels upon opening of P2X receptors by 300 µM ATP (Sigma, Taufkirchen, Germany). Glass microelectrodes were filled with 3 M KCl solution and had resistances below 1 MΩ. Two Ag/AgCl bath electrodes were used to minimize series resistance errors. Currents were recorded at a holding potential of −60 mV using a TEC-03 or a TEC-05 amplifier (npi electronics, Lambrecht, Germany), low pass filtered at 100 Hz and sampled at 200 Hz. A fast and reproducible solution exchange between different solutions was achieved by using a ~50 µl recording chamber continuously perfused at a rate of ~10 ml/min (Rettinger and Schmalzing 2003). Solutions were switched by magnetic valves under the control of Cellworks software (npi electronics, Lambrecht, Germany). All the measurements were carried out at room temperature (20−22°C). Data analysis was performed with Origin 7.5 software (OriginLab Corp., Northampton, MA, USA). Data are presented as mean ± SE from *N* experiments.

Results

Using a disulfide cross-linking approach, we have previously found that co-expression of the $P2X_1$K68C and $P2X_1$F291C mutant subunits in *X. laevis* oocytes leads to a spontaneous and specific dimer formation between the respective subunits (Marquez-Klaka et al. 2007). Likewise, expression of double mutant $P2X_1$K68C/F291C subunits leads to the formation of cross-linked trimers. K68 and F291 have been supposed to contribute to ATP binding and in agreement with this, cysteine cross-linking between co-expressed single mutant subunits and double mutant subunits was specifically prevented in the presence of ATP. Based on these findings, we have suggested that the ATP binding site is formed at the interface of two neighbouring subunits similar as in the nAChR family members. To test whether the analogous residues have a similar distance and orientation in other P2X subunits, we substituted the corresponding residues in hexahistidyl-tagged rat $P2X_2$ (K69, F289), $P2X_3$ (K63, F280) and $P2X_4$ (K67, F294) subunits by cysteine residues. In addition to the ten conserved cysteine residues in their extracellular loop (Clyne et al. 2002; Ennion and Evans 2002), $P2X_2$Rs, $P2X_3$Rs, and $P2X_4$Rs contain three, two, and four cysteine residues, respectively in their intracellular termini. Upon expression of these mutants in *X. laevis* oocytes, the P2X receptor complexes were purified under non-denaturing conditions via Ni^{2+}-NTA agarose and analysed by non-reducing SDS-PAGE analysis. To avoid unspecific multimerization and aggregation during purification or electrophoresis, iodacetamide was included throughout the protein purification. To ensure that only correctly folded, mature and functional P2X protein was visualized, we selectively labelled plasma membrane proteins by NHS-conjugated Cy5. Thus exclusively surface receptors were detected.

Cross-linking between $P2X_2$K69C and $P2X_2$F289C

Sodium dodecyl sulphate-polyacrylamide gel electrophoresis (SDS-PAGE) analysis of co-expressed $P2X_2$K69C and $P2X_2$F289C mutants under non-reducing conditions showed a spontaneous and specific formation of a band corresponding in size to a dimer (Fig. 1a, lane 4). Quantitative analysis revealed that the cross-linked fraction corresponded to 28.5 ± 3.7% of the total surface-labelled P2X protein. Significantly less (<5%) dimer formation was visible for non-mutated $P2X_2$ subunits and separately expressed single mutant $P2X_2$ subunits (Fig. 1a, lanes 1–3).

As previously observed with the corresponding $P2X_1$ mutants, the respective double mutant $P2X_2$K69C/F289C subunit was efficiently cross-linked into trimers (Fig. 1a, lane 5). Unlike what we have seen previously with the double mutant $P2X_1$ receptors (Marquez-Klaka et al. 2007), a strong monomeric band (50.6 ± 0.2% of the total P2X protein) of the $P2X_2$K69C/F289C subunits remained, indicating that the cross-linking was less effective than in $P2X_1$Rs. A faint additional band corresponding in size to a tetramer has also been observed previously and most likely represents an incompletely cross-linked trimer (Nagaya et al. 2005; Marquez-Klaka et al. 2007). In support of this interpretation, only complexes corresponding to trimers were detected by BN-PAGE analysis of metabolically labelled $P2X_1$ complexes (Marquez-Klaka et al. 2007) and $P2X_2$ complexes (not shown). Therefore we excluded that cross-linking was an artefact resulting from aggregation during the purification process.

Cross-linking between $P2X_3$K63C and $P2X_3$F280C and cross-linking between $P2X_4$K67C and $P2X_4$F294C

Co-expression of $P2X_3$K63C and $P2X_3$F280C single mutants did not lead to a significant increase in dimer formation (5.6 ± 0.7%) as compared to the separately expressed single mutants 4.6 ± 0.6 and 4.0 ± 0.9% for $P2X_3$K63C and $P2X_3$F280C, respectively (Fig. 1b, lanes 1-3). Likewise, the propensity of $P2X_4$K67C and $P2X_4$F294C single mutants to dimerize (7.8 ± 2.8 and 7.9 ± 3.0%, respectively) was not markedly increased upon co-expression (11.9 ± 1.7%, Fig. 1c, lanes 1-3). The slightly higher background in the $P2X_4$ mutants is likely due to the higher number of endogenous cysteine residues. These findings suggest that the orientation and/or distance of the critical lysine and phenylalanine residues clearly differ between P2X receptor subtypes. While a close proximity between these residues seems to be preserved in monomeric $P2X_1$ and $P2X_2$ receptors they seem to be more remote in $P2X_3$ and $P2X_4$ receptors. In an attempt to estimate the distance between these residues in $P2X_3$ and $P2X_4$ receptors we applied the homobifunctional cysteine-reactive cross-linker MTS-2-MTS (spacer length 5.2 Å, Loo and Clarke 2001). Treatment of oocytes with 0.1 mM MTS-2-MTS increased the dimer fraction to 22.3 ± 2.1% in case of the co-expressed $P2X_3$ mutants (K63C + F280C) while the background of dimer fraction in the single mutants was not markedly increased (4.3 ± 0.5% without cross-linker to 5.0 ± 0.3% with cross-linker, Fig. 1b lanes 4-6). For co-expressed $P2X_4$K67C and $P2X_4$F294C mutants, the dimer band intensity increased to 25.0 ± 0.5% (with cross-linker) in comparison to the single mutant dimer fractions of 7.8 ± 1.7% (without cross-linker) and 9.4 ± 0.5% (with cross-linker, Fig. 1c, lanes 4-6). The longer cross-linker MTS-4-MTS was also tested but unspecifically increased the dimer fraction also in the single mutants (not shown). In conclusion, a cysteine-specific cross-linking of mutated subunits was achieved with the short cross-linker MTS-2-MTS although the efficiency was

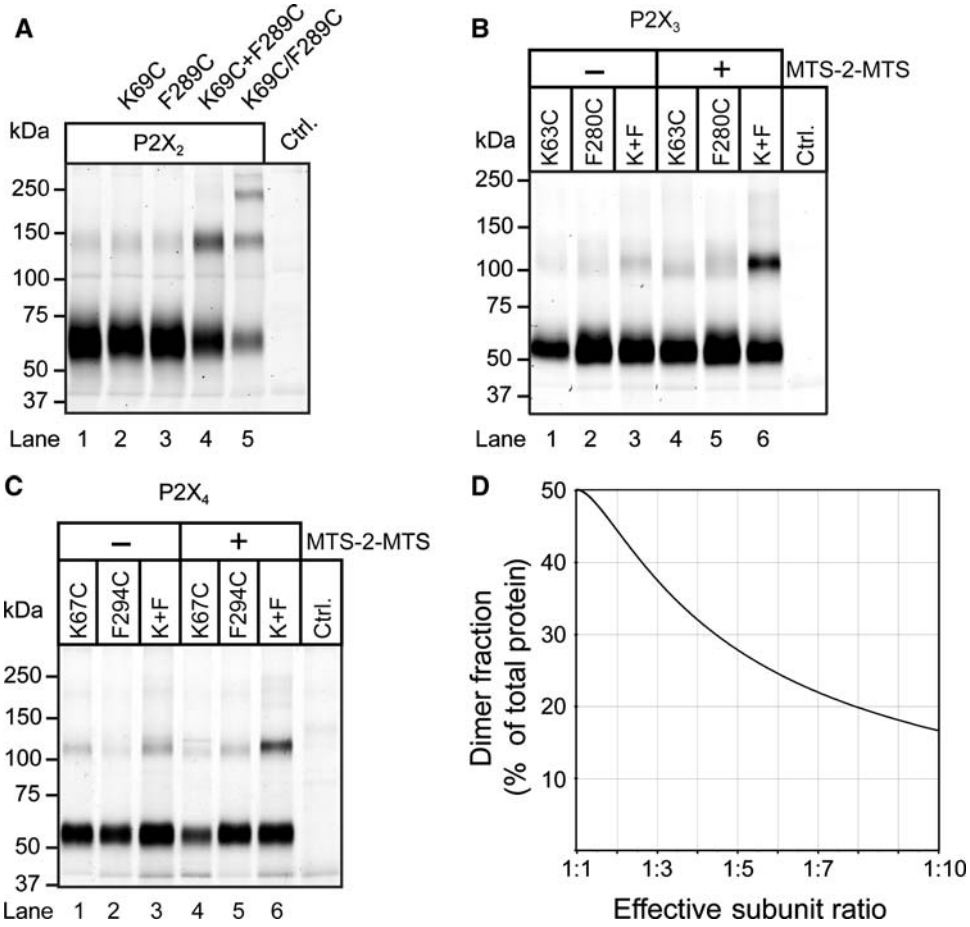

Fig. 1 Non-reducing SDS-PAGE analysis of separately and co-expressed His-P2X$_2$ (**a**), His-P2X$_3$ (**b**) and His-P2X$_4$ (**c**) mutants in which K68 and F291 residues (P2X$_1$ numbering) were substituted by cysteine residues. Intact *Xenopus laevis* oocytes injected with the indicated cRNAs and non-injected control oocytes (Control) were surface labelled by incubation in Cy5-sulfo-NHS 3 days after injection and His-tagged proteins were purified via Ni^{2+}-NTA agarose. In case of cross-linking with the cysteine-specific cross-linker MTS-2-MTS, cells were additionally incubated in MTS-2-MTS prior to purification. **d** Graphic representation of the maximal possible fraction of cross-linked dimer (as fraction of total P2X protein) depending on the effective ratio of the two mutant subunits. The maximally possible fraction of dimer was calculated assuming a binomial distribution of two mutant subunits in heterotrimeric receptors. Parameters like temporal or spatial differences in expression and plasma membrane transport of subunits are neglected. A purely stochastic assembly (and no preferential stoichiometry) and 100% complete cystine formation are assumed

lower than for the spontaneously cross-linking of P2X$_1$ and P2X$_2$ mutants.

Heteromerization of P2X$_1$ and P2X$_2$ subunits

The spontaneous dimerization of P2X$_2$K69C and P2X$_2$F289C single mutants which proceeds with similar efficiency as cross-linking between P2X$_1$K68C and P2X$_1$F291C single mutants, prompted us to investigate heteromerization between P2X$_1$ and P2X$_2$ subunits by co-expressing P2X$_1$K68C with P2X$_2$F289C single mutants and vice versa (Fig. 2a). Co-expression of P2X$_1$K68C with P2X$_2$F289C resulted in the formation of a dimer band of intermediate size (about 120 kDa, Fig. 2a lane 2), between the P2X$_1$K68C + P2X$_1$F291C dimer (100 kDa, Fig. 2a, lane 6) and the P2X$_2$K69C + P2X$_2$F289C dimer (135 kDa, Fig. 2a, lane 1). The relative amount of the heteromeric P2X$_1$K68C + P2X$_2$F289C dimer was 12.5 ± 0.2% of the total protein in comparison to background levels of 2.9 ± 0.2 and 2.9 ± 0.3% dimer formation for the negative controls P2X$_1$K68C + P2X$_2$K69C and P2X$_1$F291C + P2X$_2$F289C, respectively (Fig. 2a, lanes 3 and 5). The latter combinations should not be capable of forming a dimer by intersubunit disulfide cross-linking (Fig. 2b, schemes 3 and 5) in contrast to the P2X$_1$K68C + P2X$_2$F289C and P2X$_1$F291C + P2X$_2$K69C combinations (Fig. 2b, schemes 2 and 4). Interestingly, no significant dimerization occurred upon co-expression of P2X$_1$F291C and P2X$_2$K69C mutants (4.1 ± 1.1% dimer fraction), suggesting that P2X$_1$ and P2X$_2$ are able to heteromerize but that the interfaces between the adjoining subunits are not equivalent (Fig. 2a; lane 4, Fig. 2b).

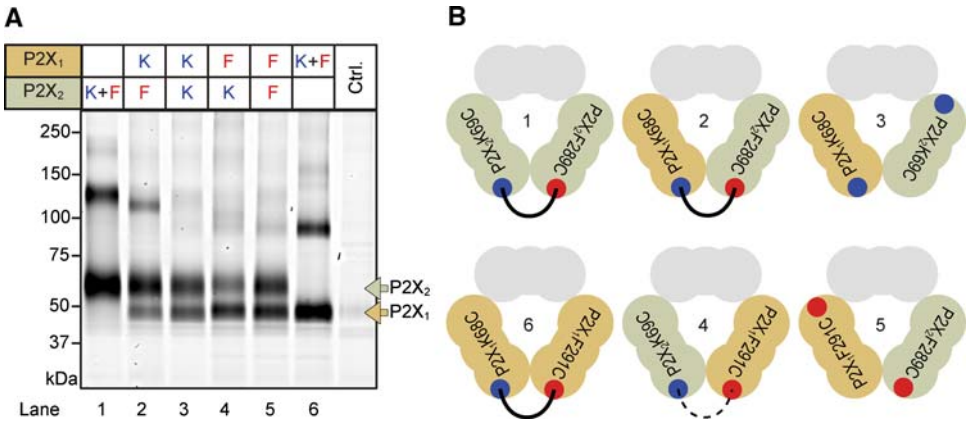

Fig. 2 Heteromerization and cross-linking between cysteine-substituted $P2X_1$ and $P2X_2$ subunits. **a** Non-reducing SDS-PAGE analysis of surface labelled $P2X_1$K68C, $P2X_1$F291C, $P2X_2$K69C, and $P2X_2$F289C mutants that were co-expressed in pair wise combinations. For clarity, cysteine-substituted lysine and phenylalanine residues are indicated as *K* and *F*, respectively. *Coloured arrows* indicate the dissociated monomeric $P2X_1$ and $P2X_2$ subunits. **b** Schematic representation of mutant heteromers and expected locations of the mutations in the co-expression experiment. *Grey shaded subunits* indicate either one of the co-expressed subunits, *blue* and *red circles* indicate cysteine-substituted lysine and phenylalanine residues, respectively and numbers correspond to lanes in (**a**). The *dotted line* indicates the non-cross-linked interface. Note that the respective homomeric complexes are not presented in the scheme

Functional analysis of the $P2X_1$-$P2X_2$ heteromer

Two-electrode voltage-clamp analysis of $P2X_1$Rs containing the K68C/F291C double mutation has shown that the disulfide cross-linked receptors are non-functional but can be rendered functional after reduction of the disulfide bond by DTT (Marquez-Klaka et al. 2007). Hence, the two cysteine substitutions do not prevent ATP binding and receptor activation unless they are forming a disulfide bond. Therefore, specific activation of cross-linked $P2X_{1/2}$ heteromers should be possible. To functionally investigate heteromerization between $P2X_1$K68C and $P2X_2$F289C subunits, two-electrode voltage-clamp analysis of receptor currents was performed in *Xenopus* oocytes. Individual expression of $P2X_1$K68C or $P2X_2$F289C subunits gave rise to the subtype-characteristic desensitizing or non-desensitizing currents, respectively (Fig. 3a, c). The desensitization time course of the $P2X_1$K68C receptor currents was biphasic and not significantly altered by DTT treatment. It could be described by the sum of two exponential functions of about equal amplitude (see Table 1). Co-expression of both mutated subunits by injection of $P2X_1$K68C and $P2X_2$F289C cRNA in equal amounts resulted in purely non-desensitizing currents (data not shown), most likely representing $P2X_2$F289C homomers. An additional desensitizing component resembling the $P2X_1$K68C homomer appeared only if $P2X_1$K68C and $P2X_2$F289C cRNAs were injected in a ratio larger than 6:1. This suggests that at $P2X_1$K68C/$P2X_2$F289C ratios below 6:1, the $P2X_1$K68C subunits co-assemble almost quantitatively with $P2X_2$F289C subunits to form heteromeric receptors. These heteromers could be either non-functional due to cross-linking or functional but resembling the non-desensitizing $P2X_2$F289C phenotype.

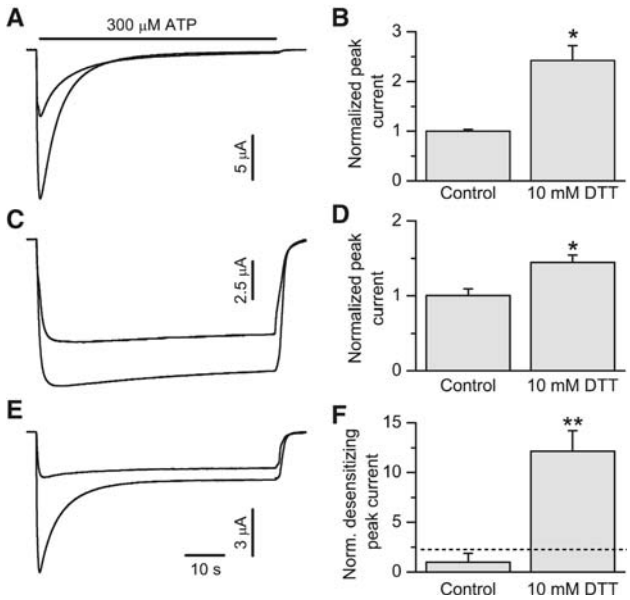

Fig. 3 Functional characterization of homomeric $P2X_1$K68C and $P2X_2$F289C and heteromeric $P2X_1$K68C/$P2X_2$F289C receptors. The *left panel* shows original current recordings from individual oocytes injected with cRNA encoding $P2X_1$K68C (**a**), $P2X_2$F289C (**c**) or both mutants (**e**) without (smaller current amplitude) and after (larger current amplitude) a 15 min pre-incubation in solution containing 10 mM DTT. The *right panel* (**b**, **d**, and **f**) shows the corresponding current amplitudes normalized to the currents before DTT treatment (mean ± SE, $N = 5$–7, * significance at $P < 0.01$ level, ** significance at $P < 0.001$ level). For **b** and **d**, total peak currents were used for analysis, while only the desensitizing component of the total current was used for analysis in **f**. The *dashed line* indicates the current level that would be expected after DTT treatment if the desensitizing part of receptor current before DTT treatment would originate from monomeric $P2X_1$K68C receptors alone

Table 1 Average receptor currents and desensitization time constants for $P2X_1K68C$, $P2X_2F289C$ and heteromeric $P2X_1K68C/P2X_2F289C$ receptors with and without DTT incubation for 15 min (±SE, $N = 5–7$)

		Control			+DTT		
	RNA ng/cell	I (μA)	τ_1 (s)	τ_2 (s)	I (μA)	τ_1 (s)	τ_2 (s)
$P2X_1K68C$	21	8 ± 0.3	3.8 ± 0.3	13.5 ± 0.6	19.4 ± 2.4	4.2 ± 0.5	11.2 ± 1.5
$P2X_2F289C$	3.5	5.6 ± 0.5	N.d.	N.d.	8.1 ± 0.6	N.d.	N.d.
$P2X_1K68C/P2X_2F289C$	21/3.5	2.85 ± 0.11	N.d.	N.d.	6.5 ± 0.5	2.6 ± 0.1	8.0 ± 0.2

Receptor currents were activated by application of 300 μM ATP at −60 mV

N.d. Not determined

To functionally resolve the $P2X_{1/2}$ heteromer, we injected $P2X_1K68C$ and $P2X_2F289C$ cRNA in the 6:1 ratio where a desensitizing component mediated by $P2X_1K68C$ homomers was virtually absent and compared currents in response to 300 μM ATP with and without a 15 min pre-incubation in 10 mM DTT. Without DTT-treatment, only 0.33 ± 0.29 μA of the total current was desensitizing (Fig. 3e, f). After DTT-treatment the desensitizing component increased more than 10-fold to 4.0 ± 0.69 μA. Again, the desensitization time course had biphasic kinetics with slightly smaller time constants as compared to homomeric $P2X_1K68C$ receptor desensitization (see Table 1). In comparison, the desensitizing homomeric $P2X_1K68C$ receptor current was increased only 2.4-fold after DTT treatment (Fig. 3a, b), while the homomeric $P2X_2F289C$ receptors remained non-desensitizing after DTT-treatment and only slightly increased in amplitude (Fig. 3c, d). Therefore, the newly appearing desensitizing component most probably represents heteromeric receptors that were rendered functional after reduction of the intersubunit disulfide bridge. Further functional characterization of the $P2X_{1/2}$ heteromer was hampered by the reduced ATP potency at the presumed binding site mutants. Marked cross-linking in heteromeric combinations containing $P2X_3$ or $P2X_4$ mutants was not oberved, most probably because of the poor propensity of these mutants to form inter-subunit cross-links.

Discussion

The conserved K68 and F291 residues ($P2X_1$ numbering) have been presumed to contribute to ATP binding in P2XRs, and we have previously shown that substitution of these residues by cysteine residues leads to a spontaneous and efficient disulfide cross-link between neighbouring $P2X_1$ subunits. Here, we substituted the corresponding lysine and phenylalanine residues in $P2X_2$ (K69, F289), $P2X_3$ (K63, F280) and $P2X_4$ (K67, F294) subunits by cysteine residues to examine whether the close proximity between these residues is preserved in other P2X receptor subtypes. We find similar results as for $P2X_1$Rs with the mutated $P2X_2$ subunits. Furthermore, we could show an interface dependent, spontaneous cross-link within heteromeric $P2X_{1/2}$Rs. In contrast, dimerization between the corresponding $P2X_3$ and $P2X_4$ mutants was clearly less efficient but was somewhat increased by treatment with a cysteine-specific cross-linker.

Efficient heteromerization between $P2X_1$ and $P2X_2$ subunits

Of the 13 biochemically identified P2XR heteromers, only 7 have also been functionally defined (for reviews see North 2002; Nicke and King 2006; Guo et al. 2007). Evidence for heteromerization between $P2X_1$ and $P2X_2$ subunits was obtained biochemically by co-immunoprecipitation (Torres et al. 1999) and BN-PAGE analysis (Aschrafi et al. 2004). A carefully conducted study by Brown et al. (2002) made use of the discriminating effects of extracellular pH to reveal functional evidence for a $P2X_{1/2}$ heteromer. Upon co-expression of $P2X_1$ and $P2X_2$ subunits in *Xenopus* oocytes, they described a current with similar agonist sensitivity and kinetics as homomeric $P2X_1$R. But in contrast to homomeric $P2X_1$Rs, the responses of the $P2X_{1/2}$ heteromer were increased at both acidic and alkaline pH and showed an overt potentiation at pH 5.5 (Brown et al. 2002). Although these data confirm the presence of a $P2X_{1/2}$ heteromer with distinct functional properties, they contrasted somewhat with independent biochemical data (Aschrafi et al. 2004) because hetero-oligomerization was inefficient and not seen in every oocyte, which hampered further pharmacological characterization.

With our biochemical approach we were able to quantify the dimer formation and show evidence for an efficient but not preferential assembly of these subunits. Reduction of the cross-linked heteromer by DTT further allowed us to specifically activate and characterize the heteromer currents. Although it has to be considered that we investigate assumed binding site mutants, our data confirm the findings of Brown et al. that the $P2X_1/P2X_2$ heteromer displays

similar desensitization kinetics as the homomeric $P2X_1R$. Furthermore, activation of heteromeric responses could be quantitatively reproduced in every oocyte studied (see Fig. 3f). Thus, similar approaches might be valuable for functionally characterizing P2X heteromers that show only subtle differences to the homomeric receptors.

Cross-linking efficiency

The efficient cross-linking in $P2X_1$ homomers (Marquez-Klaka et al. 2007), $P2X_2$ homomers and $P2X_{1/2}$ heteromers is in agreement with a conserved distance of the mutated residues and supports the idea that their direct or indirect interaction and/or distance is critical for receptor function, as for example ligand binding. The strongly reduced efficiency of cross-linking seen with homomeric $P2X_3$ and $P2X_4$ receptors, even when using bifunctional cross-linkers, might, however, indicate a larger distance at these interfaces and/or a variable orientation of the respective residues. Such diversity could account for pharmacological differences between P2X subtypes. However, the fact that both $P2X_1$Rs and $P2X_3$Rs show a quite similar pharmacology (e. g. high sensitivity to ATP and TNP-ATP) while $P2X_2$Rs more closely resemble $P2X_4$Rs in their lower sensitivity for agonists and antagonists makes this assumption less likely.

Another explanation for inefficient or absent cross-linking would be that differences in the time course of expression shifts the available ratio of mutant subunits against effective assembly and/or that different time courses of surface transport impair the appearance of cross-linked receptors in the plasma membrane. The latter has also been accounted for the slightly lower cross-linking efficiency of plasma membrane bound $P2X_1$ mutants in comparison to the total $P2X_1$ protein (Marquez-Klaka et al. 2007). Assuming (1) complete chemical reaction, (2) purely stochastic assembly (75% heteromer) and (3) equally effective plasma membrane transport of both mutants, the maximum amount of cross-linked product is 50% (2/3 of the receptor subunits are cross-linked, Fig. 1d, Marquez-Klaka et al. 2007). Relatively minor shifts in the ratio of correctly synthesized mutants and preferential surface transport of one of two mutants can therefore already account for a clearly reduced dimer fraction in membrane bound receptors (Fig. 1d). In case of heteromeric receptors, this is further influenced by the heteromerization efficiency and a possible preferential stoichiometry.

Conservation of the binding site and role of the phenylalanine in the NFR motif in receptor function

The poor cross-linking in $P2X_3$ and $P2X_4$ subtypes might also imply that one or both of the substituted residues do not contribute to the formation of a conserved ATP-binding pocket but might in fact have different functions in receptor activation. So far, most evidence for a direct involvement in ATP binding exists for the K68 residue. Alanine mutations of this residue in $P2X_1$, $P2X_2$, $P2X_3$ and $P2X_4$ subunits resulted in functionally impaired or non-responsive receptors (Wilkinson et al. 2006; Ennion et al. 2000; Jiang et al. 2000; Zemkova et al. 2007). Most convincing support for a ligand binding function of this residue has been demonstrated by single channel analysis of the K69A mutation in the background of a constitutively active $P2X_2$T339S mutant (Cao et al. 2007).

On the contrary, the function of the F291 residue is still less clear. A contribution to the coordination of ATP has originally been suggested, based on a 160-fold shift in the EC_{50} value for ATP upon mutation into alanine in $P2X_1$ (Roberts and Evans 2004) while the EC_{50} was only shifted 10-fold in a study on the analogous $P2X_4$F294A mutant (Zemkova et al. 2007). A study in which $P2X_1$ subunits with cysteine-substituted N290, F291, R292, or K309 residues were treated with MTS reagents or the photoaffinity label [^{32}P] 2-Azido ATP supports the idea that these residues are involved in agonist binding (Roberts and Evans 2007). In agreement with our hypothesis that K68 and F291 lie on opposite sites of an intersubunit binding site, a contribution of K68 and K309 from neighbouring subunits to ATP function has also been proposed (Wilkinson et al. 2006; Marquez-Klaka et al. 2007). However, evidence for a function of residues analogous to $P2X_1$K309 and a nearby segment involving G316 to I333 (in $P2X_4$) in channel gating rather than ligand binding is also accumulating (Cao et al. 2007; Yan et al. 2006).

An intersubunit binding site is reminiscent of the nAChRs. Another intriguing similarity between P2XRs and nAChRs has been proposed by Adriouch et al. (2008). Based on a study identifying ADP-ribosylation of R125 in $P2X_7$, these authors suggested that the cysteine-rich domain formed by the first six conserved cysteine residues in P2X receptors might function as a "finger-like" structure which covers the ligand binding site. This would be reminiscent of the C-loop in nAChRs. A cysteine-rich "thumb" domain has also been identified in the ASIC channel and is supposed to couple the binding of protons to the opening of the ion channel. The proton-binding site is thought to be located in a highly negatively charged cavity formed by acidic amino acid residues from adjacent subunits (Jasti et al. 2007). An attractive explanation for the variable distance of residues analogous to K68 and F291 would be that only K68 makes a direct contact with ATP while F291 is situated on a more flexible domain that moves towards the binding site upon agonist binding, or that the domains containing K68 and F291 both undergo significant movements relative to each other and that their

distance depends on the receptor subtype and/or state of the receptor.

Disulfide specific cross-linking and significance for binding site/structure determination

In the current study, a specific cysteine cross-linking was achieved with and without the addition of cross-linker in the presence of ten or more endogenous cysteines. So far, two other intersubunit cross-links between substituted cysteine residues have been identified.

In $P2X_2$, $P2X_3$ and $P2X_{2/3}$ receptors, the substitution of analogous valine and isoleucine residues located close to the extracellular side of the first and second TM, respectively, resulted in dimer formation and a loss of function that could be recovered by treatment with DTT (Spelta et al. 2003; Jiang et al. 2003). These experiments showed a "head to tail" orientation of the P2X subunits in the trimeric complex and provided evidence for a 2:1 stoichiometry of PX_3 and $P2X_2$ subunits in the heteromeric complex. The corresponding interface was also preserved in $P2X_1$Rs. Likewise, substitution of two histidine residues (H120C and H213C) in the extracellular domain of the $P2X_2$R lead to spontaneous dimer formation and non-functional receptors that were activated by reduction of the disulfide bond (Nagaya et al. 2005). As these two residues have been shown to be important for the modulatory action of Zn^{2+} at the $P2X_2$R, an inter-subunit Zn^{2+} binding site was concluded. Interestingly, the modulatory Zn^{2+} binding site in two members of the nAChR family, the glycine receptor and the γ-aminobutyric acid type A receptor, has also been located at the interface of two neighbouring subunits while both the agonist binding site and the allosteric Zn^{2+} binding site of the GluR are formed within a single subunit (Nagaya et al. 2005).

In the absence of high-resolution structural information, these cross-linking data contribute to the understanding of the subunit arrangement, heteromerization and stoichiometry as well as the relative localization of functionally important residues. Independent of the specific function of the substituted residues, they further help in mapping subunit interfaces and identifying regions that move relative to each other during channel activation. Together, this information will help the interpretation of structures and the generation of homology models for P2X subtypes once a high resolution P2XR structure becomes available.

Acknowledgments We thank Heinrich Betz for generous support and critical reading of this manuscript.

References

Adriouch S, Bannas P, Schwarz N, Fliegert R, Guse AH, Seman M, Haag F, Koch-Nolte F (2008) ADP-ribosylation at R125 gates the $P2X_7$ ion channel by presenting a covalent ligand to its nucleotide binding site. FASEB J 22(3):861–869

Aschrafi A, Sadtler S, Niculescu C, Rettinger J, Schmalzing G (2004) Trimeric architecture of homomeric $P2X_2$ and heteromeric $P2X_{1+2}$ receptor subtypes. J Mol Biol 342:333–343

Barrera NP, Ormond SJ, Henderson RM, Murrell-Lagnado RD, Edwardson JM (2005) Atomic force microscopy imaging demonstrates that $P2X_2$ receptors are trimers but that $P2X_6$ receptor subunits do not oligomerize. J Biol Chem 280:10759–10765

Brejc K, van Dijk WJ, Klaassen RV, Schuurmans M, van Der Oost J, Smit AB, Sixma TK (2001) Crystal structure of an ACh-binding protein reveals the ligand-binding domain of nicotinic receptors. Nature 411:269–276

Brown SG, Townsend-Nicholson A, Jacobson KA, Burnstock G, King BF (2002) Heteromultimeric $P2X_{1/2}$ receptors show a novel sensitivity to extracellular pH. J Pharmacol Exp Ther 300:673–680

Cao L, Young MT, Broomhead HE, Fountain SJ, North RA (2007) Thr339-to-serine substitution in rat $P2X_2$ receptor second transmembrane domain causes constitutive opening and indicates a gating role for Lys308. J Neurosci 27:12916–12923

Clyne JD, Wang LF, Hume RI (2002) Mutational analysis of the conserved cysteines of the rat $P2X_2$ purinoceptor. J Neurosci 22:3873–3880

Ennion S, Hagan S, Evans RJ (2000) The role of positively charged amino acids in ATP recognition by human $P2X_1$ receptors. J Biol Chem 275:29361–29367

Ennion SJ, Evans RJ (2002) Conserved cysteine residues in the extracellular loop of the human $P2X_1$ receptor form disulfide bonds and are involved in receptor trafficking to the cell surface. Mol Pharmacol 61:303–311

Freist W, Verhey JF, Stühmer W, Gauss DH (1998) ATP binding site of P2X channel proteins: structural similarities with class II aminoacyl-tRNA synthetases. FEBS Lett 434:61–65

Gouaux E (2004) Structure and function of AMPA receptors. J Physiol 554:249–53

Guo C, Masin M, Qureshi OS, Murrell-Lagnado RD (2007) Evidence for functional $P2X_4/P2X_7$ heteromeric receptors. Mol Pharmacol 72:1447–1456

Hansen SB, Sulzenbacher G, Huxford T, Marchot P, Taylor P, Bourne Y (2005) Structures of Aplysia AChBP complexes with nicotinic agonists and antagonists reveal distinctive binding interfaces and conformations. EMBO J 24:3635–3646

Jasti J, Furukawa H, Gonzales EB, Gouaux E (2007) Structure of acid-sensing ion channel 1 at 1.9 Å resolution and low pH. Nature 449:316–323

Jiang LH, Rassendren F, Surprenant A, North RA (2000) Identification of amino acid residues contributing to the ATP-binding site of a purinergic P2X receptor. J Biol Chem 275:34190–34196

Jiang LH, Kim M, Spelta V, Bo X, Surprenant A, North RA (2003) Subunit arrangement in P2X receptors. J Neurosci 23:8903–8910

Loo TW, Clarke DM (2001) Determining the dimensions of the drug-binding domain of human P-glycoprotein using thiol cross-linking compounds as molecular rulers. J Biol Chem 276:36877–36880

Marquez-Klaka B, Rettinger J, Bhargava Y, Eisele T, Nicke A (2007) Identification of an intersubunit cross-link between substituted cysteine residues located in the putative ATP binding site of the $P2X_1$ receptor. J Neurosci 27:1456–1466

Mayer ML (2005) Glutamate receptor ion channels. Curr Opin Neurobiol 15:282–288

Mayer ML (2006) Glutamate receptors at atomic resolution. Nature 440:456–462

Nagaya N, Tittle RK, Saar N, Dellal SS, Hume RI (2005) An intersubunit zinc binding site in rat $P2X_2$ receptors. J Biol Chem 280:25982–25993

Nicke A, King BF (2006) Heteromerization of P2X receptors. In: Arias HR (eds) Biological and biophysical aspects of ligand-gated ion channel receptor superfamilies. Research Signpost, Kerala, pp 383–418

Nicke A, Bäumert HG, Rettinger J, Eichele A, Lambrecht G, Mutschler E, Schmalzing G (1998) $P2X_1$ and $P2X_3$ receptors form stable trimers: a novel structural motif of ligand-gated ion channels. EMBO J 17:3016–3028

North RA (2002) Molecular physiology of P2X receptors. Physiol Rev 82:1013–1067

Rettinger J, Schmalzing G (2003) Activation and desensitization of the recombinant $P2X_1$ receptor at nanomolar ATP concentrations. J Gen Physiol. 121:451–461

Roberts JA, Evans RJ (2004) ATP binding at human $P2X_1$ receptors Contribution of aromatic and basic amino acids revealed using mutagenesis and partial agonists. J Biol Chem 279:9043–9055

Roberts JA, Evans RJ (2007) Cysteine substitution mutants give structural insight and identify ATP binding and activation sites at P2X receptors. J Neurosci 27:4072–4082

Schägger H, Cramer WA, von Jagow G (1994) Analysis of molecular masses and oligomeric states of protein complexes by blue native electrophoresis and isolation of membrane protein complexes by two-dimensional native electrophoresis. Anal Biochem 217:220–230

Spelta V, Jiang LH, Bailey RJ, Surprenant A, North RA (2003) Interaction between cysteines introduced into each transmembrane domain of the rat $P2X_2$ receptor. Br J Pharmacol 138:131–136

Torres GE, Egan TM, Voigt MM (1999) Hetero-oligomeric assembly of P2X receptor subunits specificities exist with regard to possible partners. J Biol Chem 274:6653–6659

Wilkinson WJ, Jiang LH, Surprenant A, North RA (2006) Role of ectodomain lysines in the subunits of the heteromeric $P2X_{2/3}$ receptor. Mol Pharmacol 70:1159–1163

Worthington RA, Smart ML, Gu BJ, Williams DA, Petrou S, Wiley JS, Barden JA (2002) Point mutations confer loss of ATP-induced human $P2X_7$ receptor function. FEBS Lett 512:43–46

Yan Z, Liang Z, Tomic M, Obsil T, Stojilkovic SS (2005) Molecular determinants of the agonist binding domain of a P2X receptor channel. Mol Pharmacol 67:1078–1088

Yan Z, Liang Z, Obsil T, Stojilkovic SS (2006) Participation of the Lys313-Ile333 sequence of the purinergic $P2X_4$ receptor in agonist binding and transduction of signals to the channel gate. J Biol Chem 281:32649–32659

Zemkova H, Yan Z, Liang Z, Jelinkova I, Tomic M, Stojilkovic SS (2007) Role of aromatic and charged ectodomain residues in the $P2X_4$ receptor functions. J Neurochem 102:1139–1150